

## Phase-sensitive above-threshold ionization of Rydberg atoms at 8 GHz

D. A. Tate, D. G. Papaioannou, and T. F. Gallagher

*Department of Physics, University of Virginia, Charlottesville, Virginia 22901*

(Received 30 April 1990)

We have observed the phase dependence of microwave above-threshold ionization (ATI) of Rydberg potassium atoms at a microwave intensity of  $3 \times 10^4 \text{ W cm}^{-2}$ . By using 5-ps pulses derived from a mode-locked tunable dye laser to create the initial Rydberg state, and phase locking the microwave field to a high harmonic of the mode-locking frequency, we are able to excite the atom at a specific phase of the microwave field. Measurement of the ejected electrons' energy as a function of the initial Rydberg state and the phase of the microwave field show that it is the phase of the field at which the electron becomes free of the atom that determines its kinetic energy. The energy dependence is described by a simple, classical theory that reveals the relationship between the so-called "quiver" and "drift" terms in the electron energy previously observed in ATI experiments at higher frequencies.

A number of recent papers have reported measurements of above-threshold ionization (ATI) in the long-wavelength, or low-frequency, limit.<sup>1-3</sup> In these measurements the observed electron-energy spectra were in agreement with a simple classical model<sup>1,2,4</sup> in which the electron's energy, in the oscillating field, is divided into two parts, a "quiver" energy and a "drift" energy. The quiver energy is the energy of oscillation of the electron in the intense oscillating field, the ponderomotive energy. This energy is converted to directed translational energy when the electron leaves the region of the oscillating field on its way to the detector. We shall assume that the field remains present until after the electron has left the region of the oscillating field. This condition is sometimes termed the long-pulse regime. The drift energy, which can be twice as large as the quiver energy, depends on the phase  $\phi$  of the oscillating field at which the electron becomes free of the atom. A critical element of this classical model is the dependence of the electron drift energy on the phase  $\phi$ , a dependence that has not been explicitly tested in the previous experiments. Here we report an explicit test of the prediction of the classical model.

The classical theory is straightforward. Consider an electron of charge  $e$  and mass  $m$  freed at time  $t_0$  with zero initial velocity into an oscillating electric field  $\mathbf{E} = \mathbf{E}_0 \sin(\omega t)$ . At any subsequent time  $t$  the velocity of the electron in the direction of the field is

$$\mathbf{v} = (e\mathbf{E}_0/m\omega)[\cos(\omega t) - \cos(\omega t_0)] . \quad (1)$$

The corresponding average velocity and kinetic energy (averaged over one cycle of the field) are

$$\langle \mathbf{v} \rangle = -(e\mathbf{E}_0/m\omega)\cos(\omega t_0) \quad (2)$$

and

$$W = \langle m\mathbf{v}^2/2 \rangle = W_p [1 + 2\cos^2(\omega t_0)] , \quad (3)$$

where  $W_p$  is just the ponderomotive energy of the electron in the field  $W_p = e^2 E_0^2 / 4m\omega^2$ . Inspection of Eqs. (2) and (3) reveals that the electron's directionality and ener-

gy are critically dependent on the phase  $\phi = \omega t_0$  at which the electron is created. In fact, the first term inside the square brackets in Eq. (3) is the quiver energy while the second term is the drift energy. The classical description above can be transformed to quantum-mechanical terms by using a wave function similar to the one given by Keldysh.<sup>5</sup>

In the experiment of Corkum, Burnett, and Brunel,<sup>3</sup> Xe atoms were ionized by picosecond pulses from an intense,  $10^{13} - 10^{14} \text{ W cm}^{-2}$ , CO<sub>2</sub> laser. Ionization was assumed to occur by the electron's tunneling out of the atom at the peak of the field so that  $\phi = \omega t_0 \approx \pi/2$ . In the experiments of Gallagher and co-workers,<sup>1,2</sup> Na atoms were excited to Rydberg states in the presence of microwave fields of up to  $3.5 \text{ kV cm}^{-1}$  (intensities of up to  $3 \times 10^4 \text{ W cm}^{-2}$ ). In this case the allowed values of  $\phi$  are determined by the requirement  $E_0 \sin\phi \geq 1/16n^4$  (in a.u.), corresponding to values of the electric field greater than the classical ionization limit for the Rydberg state excited by the laser.<sup>6</sup> For example, in a field of  $3.5 \text{ kV cm}^{-1}$  we have  $\phi \approx \pi/2$  for  $n = 18$  (corresponding to  $W \approx W_p$ ), but for  $n = 21$ ,  $\pi/4 \leq \phi \leq \pi/2$  ( $2W_p \geq W \geq W_p$ ), and at higher  $n$  we may have the electron becoming free of the atom at nearly any value of  $\phi$  between zero and  $\pi/2$  rad, giving electron energies between  $W_p$  and  $3W_p$ . States lower than  $n = 18$  may be ionized, provided  $E_0 \geq 1/3n^5$  (giving  $n \geq 14$  for  $3.5 \text{ kV cm}^{-1}$ ), by means of Landau-Zener transitions between the different Stark manifolds until the classical ionization limit is reached.<sup>7</sup> However, such electrons are most likely to become free of the atom at the peak of the field,  $\phi \approx \pi/2$ . According to this simple theory, the phase of the electric field at which the electron is freed from the atom determines the electron energies in the ATI spectra; in previous work on ATI at optical frequencies the influence of these two concepts on the electron spectra was not considered. In the earlier work on microwave ATI, long-pulse ( $\approx 5$ -ns) lasers were used to excite the Rydberg state; the laser pulse covered some 40 cycles of the 8-GHz microwave field, and so systematic investigation of the electron energy with phase was not

possible. In this paper we use the short-pulse length and temporal synchronization properties of a mode-locked laser to investigate this dependence explicitly.

The object of the experiment is to create a free electron by microwave ionization of a Rydberg state at a specific phase of the microwave field. This is possible provided that three conditions are satisfied. First, the laser pulse used to excite the Rydberg state must be much shorter than one microwave period. Second, the laser pulse and microwaves must be temporally synchronized. Third, the microwave ionization process must be effectively instantaneous (i.e., the state is ionized in less than one cycle of the field). In our experiment we use a 5-ps pulse derived from a mode-locked laser to excite the state to be ionized by an 8.2-GHz microwave field; the microwave period is  $\approx 120$  ps. The laser pulse and microwave electric field are synchronized by phase locking the microwave oscillator to a high harmonic of the rf input to the laser mode-locker head. Ionization of the Rydberg state is instantaneous if the magnitude of the microwave electric field is greater than the classical ionization limit for that state ( $1/16n^4$ ).

Other than the modifications noted in the preceding paragraph, the general idea of experiment is the same as that of Gallagher.<sup>1</sup> We excite K atoms to a point within  $600 \text{ cm}^{-1}$  of the zero-field ionization limit ( $n \geq 16$ ) in the presence of an 8.2 GHz microwave field and examine the energies of the ejected electrons by time of flight. This apparatus has been described elsewhere<sup>1,2</sup> and so its description here is brief. The source of K atoms is a horizontally directed thermal atomic beam which enters a microwave cavity via a 1-mm-diam hole in its sidewall. A counterpropagating picosecond dye laser beam enters the cavity by a similar hole in the opposite wall. The laser is tuned to the K  $4s\text{-}nd$  two-photon transitions to excite the atoms to a Rydberg state. It should be noted that the laser itself does not ionize the atom (unless it is tuned above the two-photon-ionization threshold); it merely creates the Rydberg state, which is ionized by the microwave field. A 1-mm-diam hole in the top face allows electrons liberated within the cavity to escape to the detector. On leaving the cavity the electrons enter an 8-cm-long field-free region before being accelerated into a microchannel plate (MCP) detector. The cavity works in the  $\text{TE}_{101}$  mode with its electric field vertical, and only electrons from the field antinode are observed at the detector. There is a copper septum in the center of the cavity in the plane which is perpendicular to the electric field; the field is unaffected by the presence of the septum. Biasing the septum provides a means of ejecting from the cavity low-energy electrons which would otherwise be unobservable due to the horizontal ponderomotive forces within the cavity.<sup>2</sup> We find that a small negative voltage on the septum, up to  $-8\text{V}$ , does not alter the observed electron energies once the offset due to the septum voltage is accounted for. The resonant frequency of the cavity is tuned to that of the phase-locked microwave oscillator by means of a tuning stub in the endwall which effectively changes the cavity length, giving a tuning range of  $\approx 100$  MHz. The cavity is tuned to a resonant frequency of 8.197 12 GHz (determined by the phase

locking; see below) where it has a  $Q$  of 930. The microwave source is a Hewlett Packard (HP) model 8350B/83550B sweep oscillator and plugin which is amplified by a Litton 624 traveling-wave tube amplifier, which is gated on for  $1 \mu\text{s}$  at each laser pulse. Between the oscillator and amplifier there is a HP model 8494B 0–11-dB variable attenuator and a HP model X855A variable phase shifter. From the amplifier the microwave power passes through a 20-dB waveguide coupler, which allows the power to be monitored by a HP model 432 power meter. The power is then coupled into semirigid coaxial cable and through a circulator which allows the reflected microwave power to be monitored. Microwave power drifts were monitored on a day to day basis by measuring the microwave ionization thresholds of the K  $14d$ ,  $15d$ , and  $16d$  states in a similar fashion to that described by van Linden van den Heuvell and Gallagher.<sup>7</sup> The uncertainty in the microwave power calibration is 15%.

The laser system used in this experiment is based on a synchronously pumped mode-locked dye laser [Coherent model 701-2 pumped by the second harmonic of an Antares 76-S mode-locked Nd:YAG laser (where YAG is yttrium aluminum garnet)] operating at 76 MHz. The out-

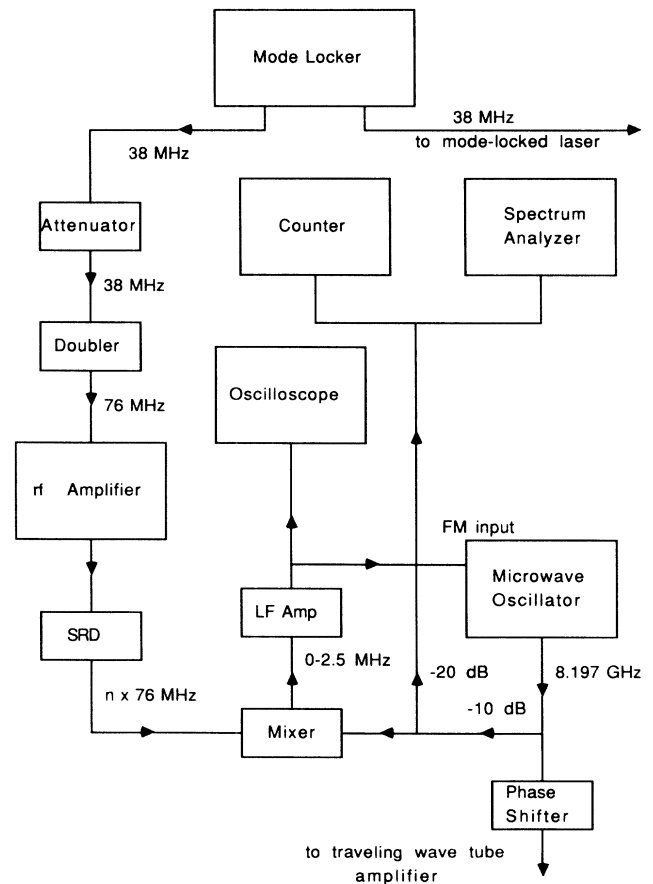


FIG. 1. Outline of microwave phase-locking scheme. SRD is the step-recovery diode, LF Amp is the low-frequency amplifier, FM input is the frequency modulation input port to microwave oscillator, rf is radio frequency.

put of the dye laser is then amplified in a three stage dye amplifier (Continuum PTA10) pumped by the frequency doubled output of a Nd:YAG regenerative amplifier (Continuum RGA60-20). The final output of this system is  $\approx 0.5$  mJ in a 5.0-ps [autocorrelation full width at half-maximum (FWHM) is 7.8 ps;  $\text{sech}^2$  pulse shape assumed] pulse at a repetition rate of 20 Hz. With rhodamine 6 G (rhodamine 590) in both the dye oscillator and amplifier, the system is tunable over the range 560–590 nm. This tuning range is sufficient to excite K  $nd$  states of  $n \geq 11$  by two-photon excitation.

As the laser system is based on an actively mode-locked Nd:YAG laser, synchronization of the laser pulse and microwave field is, in principle at least, relatively straightforward. A diagram of our microwave phase-locking scheme is shown in Fig. 1. The mode-locking frequency is the internal clock of this experiment; in our case this frequency is 38 MHz. This 38-MHz field produces a power-dependent standing-wave pattern within a quartz prism situated inside the Nd:YAG mode-locked laser cavity. In effect this constitutes a shutter which opens and closes at twice the 38-MHz input frequency; for optimum mode locking this is also the inverse of the time it takes a photon to make one round-trip through the laser cavity. If we assume that the laser is at this optimum condition, the output pulse of the laser will always appear at a specific phase of a 76-MHz field which is phase locked to the 38-MHz output of the mode locker. This statement will also be true for a field which is any even harmonic of 38 MHz and which is phase locked to the mode-locker field. Since the dye laser is synchronously pumped by the Nd:YAG laser, its output pulses will also be synchronized with the mode-locker field, even when amplified by the dye amplifier. Phase locking of the microwave field to the 38-MHz output of the mode locker is achieved in the following way. We take one of the 38-MHz auxiliary outputs of the mode-locker driver and attenuate it before passing it into a Mini-Circuits FK-5 doubler. The doubler output is then filtered to remove as far as possible any residual 38 MHz and any frequencies above 76 MHz. The doubled rf is then amplified in a 3W 250-kHz–110-MHz power amplifier, filtered again, and passed through a step-recovery diode [(SRD), HP 5082-0820]. The SRD produces a “comb” of output frequencies at multiples of the 76-MHz input frequency beyond 8 GHz. We chose the frequency which fell in the tuning range of the cavity, 8.197 12 GHz, corresponding to the 216th harmonic of the 37.9496-MHz output of the mode-locker driver, to which to phase lock the sweep oscillator. To lock the oscillator, we mix a small amount, 5 mW, of the oscillator output with the total spectral output of the SRD in a Watkins-Johnson M31A mixer; the low-frequency beat is then amplified in a 0–2.5-MHz, 10-dB amplifier (Analog Devices 524) and fed into the FM input port on the sweep oscillator. The low-frequency amplifier acts as a filter; only the beat between the sweep oscillator and the nearest order of the SRD output is fed back into the oscillator. We monitor the beat on an oscilloscope and the sweep oscillator spectrum and frequency using a Tektronix (TEK) 2754 21-GHz spectrum analyzer and HP 5343A counter, respectively. Using these diagnostics, we are able to moni-

tor the quality of the phase locking; we estimate that the oscillator is locked to the 216th harmonic of the mode-locker frequency to  $\approx 3^\circ$ , which is less than the  $6^\circ$  subtended by the 5-ps-long pulse at 8.2 GHz. The major source of phase uncertainty in this experiment is due to the 10–15-ps jitter of the pulse from the mode-locked Nd:YAG laser, corresponding to a  $30^\circ$ – $45^\circ$  phase uncertainty at 8.2 GHz.

The microwave cavity and electron spectrometer are enclosed in a 0.25-mm-thick CoNetic magnetic shield which reduces the magnetic field to  $< 50$  mG. The resolution of the electron spectrometer is  $\approx 0.8$  eV at an energy of 10 eV. The output signal from the MCP is fed to a 0.1–1300-MHz, 20-dB amplifier (HP 8447F) and then to a digital oscilloscope (TEK 2430). The averaged spectrum of 256 laser shots is then passed to a minicomputer.

The electron time-of-flight spectra when the microwaves are unlocked are shown in Fig. 2 for three laser tunings which correspond to the excitation of the  $16d$ ,  $20d$ , and  $(42-46)d$  states in zero field. For simplicity we shall refer to these excitations as to the  $16d$ ,  $20d$ , and  $(42-46)d$  states, although it is clear that  $l$  is not a good quantum number in the field. These states are chosen so that in a field of  $\approx 3.6$  kV  $\text{cm}^{-1}$ , the  $16d$  state will ionize only at the peak of the microwave field ( $\phi \approx \pi/2$ ), the  $20d$  state anywhere between (approximately)  $\phi = \pi/4$  and  $\pi/2$ , and the  $(42-46)d$  states at virtually all phases of the field. [The laser does not have sufficient resolution to excite a single  $n$  state for  $n \geq 25$  due to the large bandwidth of the picosecond pulse ( $\approx 6$   $\text{cm}^{-1}$ ), corresponding to a coherent width of  $\approx 10$   $\text{cm}^{-1}$  in a two-photon transition; at  $n = 44$  the spacing of  $n$  levels is  $2.6$   $\text{cm}^{-1}$ . However, this limitation does not affect the results of the experiment.] The data of Fig. 2 reproduce the results of Gal-

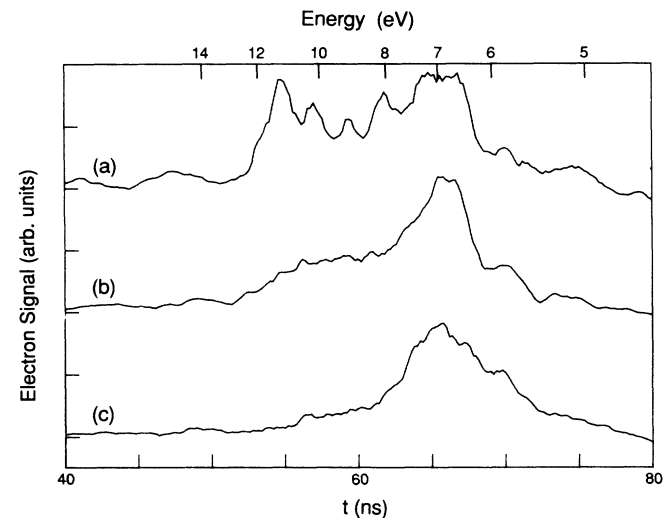


FIG. 2. Electron time-of-flight spectra due to microwave ATI for various Rydberg states for a microwave intensity of  $33$   $\text{kW cm}^{-2}$  ( $3.5$   $\text{kV cm}^{-1}$ ;  $W_p = 2.1$  eV) when the microwaves are unsynchronized: (a)  $n = (42-46)d$ , (b) the  $20d$  state, and (c) the  $16d$  state. Note offset of 4 eV on energy scale due to septum voltage of  $-8.0$  V.

lagher and Scholz,<sup>2</sup> as we expect. The ranges of electron energies seen is also what we would expect on the basis of the foregoing argument ( $W_p \leq W \leq 3W_p$ ) once the spectrometer resolution and microwave power calibration uncertainty have been considered.

Figure 3 shows the total electron yield (energies  $> 4$  eV) versus the phase shift introduced by the phase shifter when the laser is tuned just below the ionization limit. In Fig. 3(a) the microwaves are unlocked and no phase dependence of electron yield is found. However, Fig. 3(b) shows the same situation with the microwaves locked; electrons are seen at the detector only at specific phases of the field. This result may be explained with reference to Eq. (2); for half the microwave field cycle the electric field pushes the electrons in the direction opposite to that of the detector, and they cannot be observed. The values of  $\phi = \omega t_0$  assigned with reference to Eq. (2) are shown at the top of Fig. 3(b).

We present the phase  $\phi = \omega t_0$ , which we assign on the

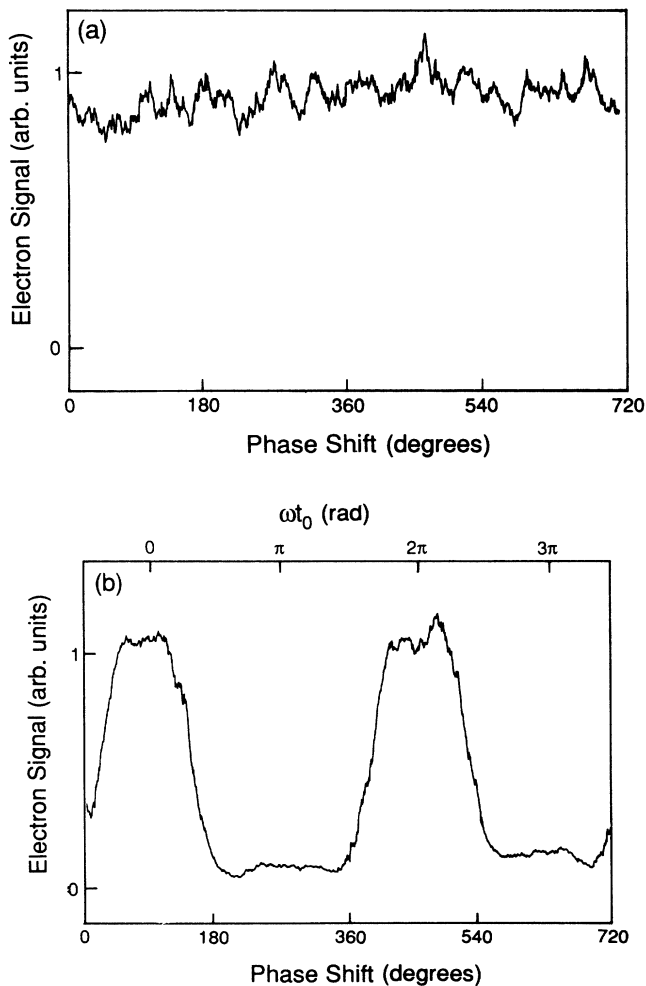


FIG. 3. Electron yield (energies greater than 4 eV) as a function of phase shift when the laser is tuned to just below the ionization limit and (a) the microwaves are unlocked, (b) locked. Septum voltage is  $-0.5$  V. The values of the phase  $\omega t_0$  assigned using Eq. (2) are given at the top of the figure.

basis of Eq. (2), or later Eq. (3), in radians to distinguish it from the measured phase shift, which is given in degrees. We must bear in mind that we have no way to measure the absolute phase shift, so all the measured phase shifts are relative to an unknown but fixed phase. Figures 4(a)–4(c) show the variation of the electron-energy spectrum with phase shift introduced by the phase shifter for the three initial Rydberg states in a microwave field of  $3.5$   $\text{kV cm}^{-1}$ , corresponding to  $W_p = 2.1$  eV. Figure 4(a) shows the electron-energy spectrum when the  $16d$  state is excited by the laser. The  $16d$  state ionizes only at the peak of the field, giving electrons of energy equal to the ponderomotive potential. There is no phase dependence of the electron energy, nor is there any change in the energy distribution when the microwaves are unlocked. In Fig. 4(b), showing the electron-energy spectrum when the  $20d$  state is excited, it can be seen that there is a change in the electron-energy distribution with phase. As the phase shift increases from  $0^\circ$  to  $90^\circ$ , the high-energy electrons disappear leaving only electrons with energy equal to the ponderomotive potential. For phases between  $90^\circ$  and  $180^\circ$  the electrons are restricted to low energies, but for phase shifts between  $210^\circ$  and  $300^\circ$  it can be seen that the high-energy wing of the distribution reappears and the low-energy peak becomes much less distinct. As the phase shift increases further the energy spectrum of the electrons again retreats to a single peak at  $W_p$ . For reference, on the right-hand side we assign the values of  $\omega t_0 = 0$  and  $-\pi$ , using the fact that when  $\omega t_0 = 0$  the highest energy electrons are detected and that at  $\omega t_0 = \pm\pi$  the minimum number of electrons are detected. Note that  $\omega t_0$  changes by  $2\pi$  and the time of flight spectrum repeats in  $300^\circ$  of phase shift, not  $360^\circ$ , due to thermal drifts in the cavity length of the mode-locked Nd:YAG laser, which alters the phase of the microwave field at which the laser pulse excites the atoms. Over the 20-min period required to complete the scans of Figs. 4(b) and 4(c) the effect of the thermal drift is quite evident. However, the data of Fig. 3(b), taken in 2 min, are unaffected by thermal drift and clearly show a period of  $360^\circ$  in the phase shift. It should be noted that the range of electron energies mapped out as the phase is changed is just the same as that when the microwave field is unlocked (top trace).

The change in electron energy with phase is even more dramatic for  $n = (42-46)d$  [Fig. 4(c)]; the peak energy oscillates between  $W_p$  and  $3W_p$  with a period of approximately  $2\pi$  in the manner predicted by Eq. (3) as the phase shift is changed. As in Fig. 4(b) we can assign the correct values of the phase  $\phi$  by noting the phase shift  $210^\circ$  at which we observe electrons of maximum energy ( $\phi = 0$ ). The phase can be independently determined from Fig. 3(b) using Eq. (2). At phase shifts from  $60^\circ$  to  $90^\circ$  the signal vanishes due to the electrons' being ejected down and hitting the septum. Thus the phase  $\omega t_0 = -\pi$  as indicated. At a phase shift of  $360^\circ$  the electron signal again vanishes since the electrons are ejected down, and the phase  $\omega t_0 \approx \pi$ . The phase values assigned in this way are shown in the right-hand margin. As in Fig. 4(b), the period of the energy oscillation appears to be less than  $360^\circ$  due to

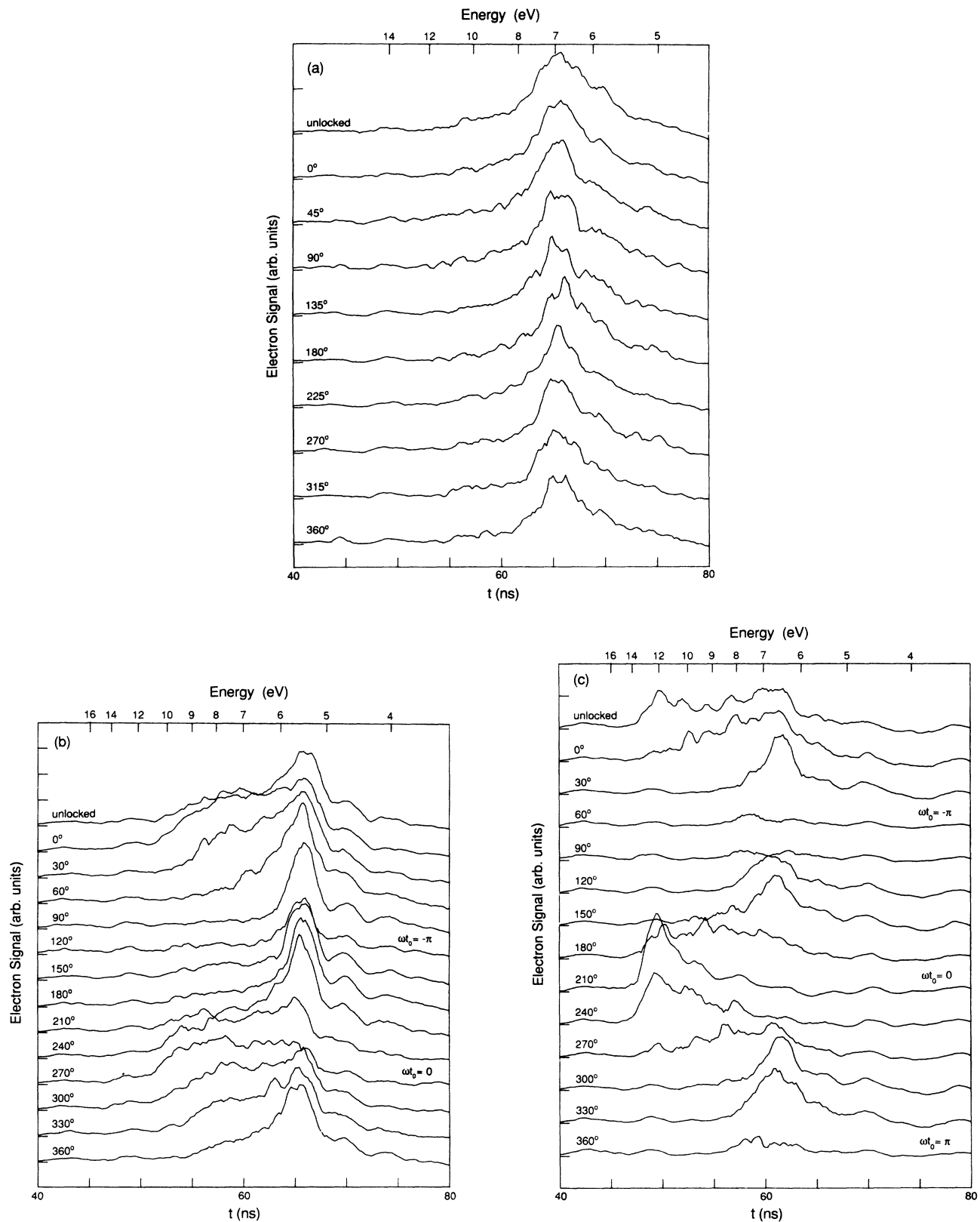


FIG. 4. Electron time-of-flight spectra as a function of phase shifter setting for the excitation of the (a)  $16d$ , (b)  $20d$ , and (c)  $(42-46)d$  states when the microwaves are phase locked. In each case the time-of-flight spectrum with the phase unlocked is shown in the uppermost trace for comparison. The phase shift in degrees is given at the left-hand side of each trace. The approximate phase angle  $\omega t_0$  in radians is given on the right-hand side in (b) and (c). There is no phase dependence in (a), thus we are unable to assign values of  $\omega t_0$ . Note that the electron energies are not corrected for the septum voltage of  $-8.0$  V. Thus the observed energies are 4 eV higher than expected on the basis of the microwave field alone.

thermal expansion of the laser cavity, which changes the phase of the laser pulse with respect to the microwave field.

Two further points should be made. First, the interval where the signal vanishes due to the electron's being ejected in the direction opposite to that of the detector is much smaller than  $180^\circ$ , an effect more easily apparent in Figs. 4(a) and 4(b). The reason for this is that putting a voltage on the septum so that low-energy electrons can escape from the cavity also changes the direction of downward directed, low-energy electrons. With no septum voltage, these would not be detected as Fig. 3(b) clearly shows. Second, as mentioned above, the width of the electron peaks is determined by the comparatively low resolution of our spectrometer and the temporal jitter of the laser pulse. Again, the limits of the energy envelope are the same as those when the laser and microwaves are not synchronized. Further, Figs. 4(b) and 4(c) show the size of the electron signal varying in the way predicted by Gallagher<sup>1</sup> and the change in the peak widths changes as we would expect when a fixed time interval is convoluted into Eq. (2).

This experiment explicitly confirms the validity of the classical model proposed to explain ATI in the long-wavelength or low-frequency limit. In addition, it shows that it is possible to determine the phase of the microwave field at which the electron becomes free of the atom. For example, Fig. 4(a) shows that when the atoms are excited to the  $16d$  state, the electrons are only freed from the atom at the peak of the ionizing field, irrespective of the phase at which they are excited. The atoms make transitions to a higher state  $n \approx 19$  before ionizing. In contrast, when the atoms are excited to the  $n = 20d$  state, some atoms can be directly ionized from the  $20d$  state in fields as low as  $1/16n^4$ , which corresponds to a microwave phase of  $16^\circ$ . As a result, when  $\phi \geq 16^\circ$ , some

of the atoms can ionize instantly, leading to the observed variation of the electron-energy spectrum with phase shown in Fig. 4(b). Due to the distribution of states excited by the laser, not all the atoms can ionize at  $E = 1/16n^4$ , and as a result, the high-energy end of the electron-energy spectrum is not as pronounced as if there existed a sharp threshold field at  $1/16n^4$ . Finally, when the  $n = (42-46)d$  states are excited, the atoms can be ionized at phases  $> 4^\circ$ , so ionization occurs immediately upon excitation, irrespective of the phase, and there is a pronounced dependence of the electron energy on the phase as shown by Fig. 4(c).

On a more fundamental level, this work indicates that the ATI spectrum is different for ionization which occurs over many rather than one cycle of the ionizing field. In the optical  $1.06\text{-}\mu\text{m}$  and  $532\text{-nm}$  ATI experiments many cycles of the field are required, leading to well-resolved ATI electron-energy peaks, separated by the photon energy, and resonances in short pulse experiments.<sup>8</sup> On the other hand, the phase dependence of these experiments clearly indicates that an 8-GHz ionization occurs at a well-defined phase of a single cycle by field ionization. As a consequence, the ATI spectrum may be used to infer the mechanism of ionization. It would be most interesting to do the experiment with radiation of intermediate wavelength with enough energy resolution to observe the transition between the two regimes.

It is a pleasure to acknowledge stimulating discussions with L. G. Wang, H. G. Muller, and H. B. van Linden van den Heuvell. This work is supported by the Air Force Office of Scientific Research under Grant No. AFOSR-90-0036, the National Science Foundation, and Strategic Defense Initiative Office of Innovative Science and Technology under the direction of the Naval Research Laboratory.

<sup>1</sup>T. F. Gallagher, Phys. Rev. Lett. **61**, 2304 (1988).

<sup>2</sup>T. F. Gallagher and T. J. Scholz, Phys. Rev. A **40**, 2762 (1989).

<sup>3</sup>P. B. Corkum, N. H. Burnett, and F. Brunel, Phys. Rev. Lett. **62**, 1259 (1989).

<sup>4</sup>H. B. van Linden van den Heuvell and H. G. Muller, in *Proceedings of the Fourth International Conference on Multiphoton Processes, Boulder, Colorado, 1987*, edited by S. J. Smith and P. L. Knight (Cambridge University Press, Cambridge, 1987).

<sup>5</sup>L. V. Keldysh, Zh. Eksp. Teor. Fiz. **47**, 1945 (1964) [Sov. Phys.—JETP **20**, 1307 (1965)].

<sup>6</sup>P. Pillet, W. W. Smith, R. Kachru, N. H. Tran, and T. F. Gallagher, Phys. Rev. Lett. **50**, 1042 (1983).

<sup>7</sup>H. B. van Linden van den Heuvell and T. F. Gallagher, Phys. Rev. A **32**, 1495 (1985).

<sup>8</sup>R. R. Freeman, P. H. Bucksbaum, H. Milchberg, S. Darack, D. Schumacher, and M. E. Geusic, Phys. Rev. Lett. **59**, 1092 (1987).